OSCILLATORY MODES OF BEHAVIOR IN A SIMPLE MODEL OF THE ATLANTIC THERMOHALINE CIRCULATION

K.Sakai and W.R.Peltier
Department of Physics
University of Toronto
Toronto, ONT
CANADA, M5S 1A7

ABSTRACT

A two-dimensional spherical model of the thermohaline circulation has been constructed that may be integrated both with and without the use of a convective adjustment scheme in order to simulate the internal variability that may be characteristic of the overturning flow. The behavior of the model is governed by several nondimensional control parameters: thermal and haline Rayleigh numbers, Prandtl number, Lewis number, and the ratio of horizontal and vertical diffusivities. Mixed boundary conditions are employed in our analyses as in previous studies based upon somewhat different model systems.

Our focus in the analyses with the new model is on the nature of the internal variability that is supported when the two Rayleigh numbers are set to sufficiently high values so as to induce a mean circulation which matches that of the modern Atlantic basin. Our purpose is to understand whether the internal variability exhibited by the model in this region of parameter space might bear any resemblance to the long term variability of climate in the North Atlantic that has been inferred on the basis of the analysis of oxygen isotopic records from Greenland ice cores, one component of which has come to be known as the "Dansgaard-Oeschger oscillations"(Dansgaard et al.,1984, Oeschger et al.,1984).

1. INTRODUCTION

Since first publication of the superb isotopic records from Vostok (Lorius et al.,1985) revealing the detailed nature of the long timescale climate oscillation accompanying the most recent ice age cycle of late Pleistocene time, many additional paleoclimatological analyses have added further detail to our understanding of this period. Other than Antarctic ice cores, deep sea sedimentary cores, pollen records, Greenland ice cores, and many other records all support the notion that the dominant time scale of climatic variability has occurred on the period of the ice age cycle itself (100 kyr. 1 kyr = 1000 years) with additional marked concentrations of spectral power at the periods of 41 kyr,and 19, 21 and 23 kyr as expected on the basis of the Milankovitch theory of orbitally induced climatic change (e.g. Hyde and Peltier, 1987). Paleorecords providing much higher resolution time series than those

NATO ASI Series, Vol. I 12
Ice in the Climate System
Edited by W. Richard Peltier

from the Vostok ice core or of deep sea sedimentary cores have also revealed the existence of variability on timescales much shorter than can be understood in terms of insolation variations associated with changes of the parameters that determine the geometry of the earth's orbit around the sun. Dansgaard et al.(1984), for example, demonstrated that the oxygen isotopic record from Greenland ice cores during the last 8.5 kyr displays variability in the period range from 2.5 kyr to 1.1 kyr, an episodicity that has since come to be called the Dansgaard-Oeschger oscillation. Stuiver(1980) has also demonstrated that the power spectra of various paleorecords over the last millennium have common spectral maxima at periods ranging from decades to centuries, and Neftel et al.(1981) showed that the spectrum of a La Jolla tree ring $\delta^{14}C$ record has a millennium scale oscillation as well as century scale features.

In addition to these oscillatory climatic variations, there have also occurred a number of rather abrupt events within individual ice age cycles, including of course the sharp terminations (Broecker and Van Donk, 1970) that mark the end of each 100 kyr pulse. The last deglaciation event has been studied in considerable detail and it is now well known that this event was interrupted by the so called Younger-Dryas period during which deglaciation was temporarily arrested for a reason that is as yet not entirely understood. Both stable carbon isotopic records and Ca/Cd records from Atlantic deep sea cores (e.g. Boyle and Keigwin,1987; Charles and Fairbanks,1991), have demonstrated that very rapid and profound changes of the deep ocean circulation are strongly correlated with the onset and termination of the Younger-Dryas event.

In order to better understand the origins and nature of these climate variations a wide variety of modeling studies have been performed. General circulation models(GCMs), in particular, have been employed to reconstruct paleoclimatic conditions at various times in the past (e.g. Manabe and Broccoli,1985; Kutzbach and Guetter,1986). Simplified climatic models featuring some subset of processes such as ice sheet growth/retreat and isostatic adjustment of the bedrock (e.g. Deblonde and Peltier,1991), and various dynamical systems models (e.g. Saltzman,1987; Ghil and Le Treut,1981) have also been used to investigate the temporal variability of climate on such very long timescales. As computational power continues to increase, models containing progressively more detailed representations of the full climate system will doubtless be employed to understand the full range of mechanisms of climatic variability that the natural system supports.

Considering the variability of climate on the range of timescales mentioned above, from decades to millennia, the oceans are expected to play a rather important role. This component of the climate system is clearly a critical agent in biogeochemical cycles, given its role as reservoir for both heat and water substance and as a transporter of heat that is as important as that of the atmosphere itself. The deep ocean circulation also influences the atmospheric concentrations of greenhouse gases through both chemical and physical processes, and the fact that the heat transported by the ocean meridionally is as large as that by the atmosphere means that any significant change in the ocean circulation may strongly affect global climate.

Although many three dimensional Ocean GCMs have been constructed for climate studies, they are still impractical for use in the extremely long timescale integrations that are required to understand the physics of long timescale climate variability (on the timescale of the ice age cycle, for example). When we focus on the behavior of the oceans on the longest timescales, spatially and temporally small scale processes might reasonably be parameterized in terms of the large scale fields and on these largest timescales we expect that the thermohaline circulation will dominate the system. There have of course been many modeling studies directed towards the development of a better understanding of the physics of the thermohaline circulation since the original box model analyses of Stommel(1961). An interesting feature of this component of the ocean circulation is that it allows the existence of multiple equilibria. These have been explored using the "box" models of Stomell(1961), the more realistic but still heavily parameterized models of Marotzke(1988) and Wright and Stocker(1991), with the more complete hydrodynamic models of Thual and McWilliams(1992) and Cessi and Young(1992) and with full OGCM's by, e.g., Bryan(1986). Winton and Sarachik(1993) have demonstrated with both their two and three-dimensional hemispheric single basin models that the possibility exists of self-sustaining oscillations of the thermohaline circulation similar to those previously revealed in the OGCM simulation of Mikolajevicz and Meier-Reimer(1990).

There are, however, considerable disagreements among the proponents of the various simplified models listed above, a clear reflection of the fact that the physics of the thermohaline circulation has yet to be fully understood. In the discussion to follow we shall present a "purely convective" thermohaline model that we think may be able to contribute usefully to the development of a better understanding of the dynamics of this process. In the next section the details of this model will be presented, while the numerical sensitivity tests performed with it are described in section 3. The results of our initial experiments are presented in section 4.1 for simulations in which no convective adjustment scheme is employed, and in section 4.2 with convective adjustment included. Following a brief discussion of these results in section 5, concluding remarks, along with a discussion of the prospects for further development of the model, are presented in section 6.

2. MODEL DESCRIPTION

A two-dimensional model has been developed to investigate the basic physics of the thermohaline circulation. The model domain consists of a thin spherical shell and the dynamical equations are comprised of the zonally averaged primitive equations, with colatitude θ and radial position r as independent spatial coordinates. The field variables on which the dynamical system is based consist of temperature T, salinity s, and velocity $\boldsymbol{u}$. In the Boussinesq approximation and employing a formulation in terms of streamfunction ψ and zonal vorticity ω, neglecting the inertia terms(Hasselman, 1982), the field equations reduce to:

$$\nu \triangle_{\nu} \omega = -\frac{g}{\rho r_0} \frac{\partial \rho}{\partial \theta} \tag{1}$$

$$\left(\frac{\partial^2}{\partial r^2}+\frac{1}{r^2}\frac{\partial^2}{\partial\theta^2}-\frac{\cot\theta}{r^2}\frac{\partial}{\partial\theta}\right)\psi = -(r\rho_0\sin\theta)\omega \quad (2)$$

$$\frac{DT}{Dt} = K_T\triangle_T T \quad (3)$$

$$\frac{Ds}{Dt} = K_s\triangle_s s. \quad (4)$$

In the above system we have furthermore ignored Coriolis effects and so are assuming that the gyre transport caused by surface wind stress may be reasonably expressed by a diffusive parameterization. As a result of these assumptions, the zonally averaged system is identical to an axially symmetric convection model which requires no parameterization of the longitudinal pressure difference.

From observational estimates of diapycnal mass transport by Olbers et al.(1985) for the North Atlantic Ocean, the effective diffusivity is much less than $10^{-4}[\mathrm{m}^2/\mathrm{s}]$ over most of the deep ocean, and we shall therefore employ the value $K_{Tv}=10^{-5}[\mathrm{m}^2/\mathrm{s}]$ for the vertical thermal diffusion coefficient. This value is somewhat smaller than the values employed by others, yet considerably larger than the molecule diffusivity, a clear indication that the diffusion process is turbulent in nature so that the Lewis number Le, the ratio of haline to thermal diffusivity, may be close to unity (a value we shall assume hereafter unless explicitly mentioned). The horizontal "diffusion" of heat and salt occurs mainly through mesoscale eddies and gyretransport, and we shall assume these processes to occur on a much faster timescale than vertical diffusion. Although these coefficients could be parameterized in terms of a Richardson number, we shall rather employ a simple uniform diffusivity. The results to be reported in what follows were computed with $\epsilon_K \equiv \frac{K_{Th}}{K_{Tv}} = 3\times 10^7$ as the ratio between horizontal and vertical thermal diffusivity.

There is no satisfactory *a priori* criterion on the basis of which we may specify the absolute value of the horizontal momentum diffusivity yet we are obliged to specify the ratio of horizontal/vertical viscosity in order to integrate the dynamical system. In order to investigate the impact on the physics of the thermohaline circulation, we have therefore carried out a series of experiments using different values of $\epsilon_\omega = \frac{\nu_h}{\nu_v}$, ranging from 3×10^7 to 3×10^3. Hereafter we shall omit the subscripts v and h on the different diffusion coefficients, choosing rather to denote these differences using the vertical component and the ratio between the vertical and horizontal components for each coefficient.

We may nondimensionalize the above dynamical equations by employing the scales:

$$t = \tau t_* = \frac{L_z^2}{K_{Tv}} \quad (5)$$

$$r = L_y r_\dagger = L_z r_* = L_y + L_z H_*(z_*-1) \quad (6)$$

in which L_z is a representative depth of the ocean and L_y is the radius of the earth. The ratio $\epsilon_r^2=(\frac{L_z}{L_y})^2$ is somewhat larger than ϵ_K^{-1}. Temperature and salinity are nondimensionalized as:

$$T = T_c T_* + T_0 \quad (7)$$

$$s = s_c s_* + s_0 \tag{8}$$

$$T_c = \frac{\nu K_T}{g\alpha L_z^3 \epsilon_r^2} \tag{9}$$

$$s_c = \frac{\nu K_T}{g\beta L_z^3 \epsilon_r^2} \tag{10}$$

$$\epsilon = \epsilon_K \epsilon_r^2. \tag{11}$$

Velocity related quantities are:

$$\psi = \frac{\rho_0 L_y^2 L_z}{\tau} \psi_* \tag{12}$$

$$\omega = \frac{1}{\epsilon_r \tau} \omega_*. \tag{13}$$

In terms of these nondimensional variables, the governing equations become:

$$\frac{\partial T_*}{\partial t_*} = J_0 J_*(\psi_*, T_*) + \triangle_T^* T_* \tag{14}$$

$$\frac{\partial s_*}{\partial t_*} = J_0 J_*(\psi_*, s_*) + \frac{1}{Le} \triangle_s^* s_* \tag{15}$$

$$\triangle_\omega^* \omega_* = \frac{1}{r_\dagger} \frac{\partial \rho_*}{\partial \theta} \tag{16}$$

$$\triangle_\psi^* \psi_* = -(r_\dagger \sin\theta)\omega_*, \tag{17}$$

in which

$$\triangle_T^* = \frac{1}{H_*^2}\frac{\partial^2}{\partial z_*^2} + \frac{1}{r_* H_*}\frac{\partial}{\partial z_*} + \frac{\epsilon}{r_\dagger^2}\frac{\partial^2}{\partial \theta^2} + \frac{\epsilon \cot\theta}{r_\dagger}\frac{\partial}{\partial \theta} \tag{18}$$

$$\triangle_s^* = \frac{1}{H_*^2}\frac{\partial^2}{\partial z_*^2} + \frac{1}{r_* H_*}\frac{\partial}{\partial z_*} + \frac{\epsilon Le}{r_\dagger^2}\frac{\partial^2}{\partial \theta^2} + \frac{\epsilon Le \cot\theta}{r_\dagger}\frac{\partial}{\partial \theta} \tag{19}$$

$$\triangle_\omega^* = \frac{1}{H_*^2}\frac{\partial^2}{\partial z_*^2} + \frac{1}{r_* H_*}\frac{\partial}{\partial z_*} + \frac{\epsilon Pr_h}{r_\dagger^2}\frac{\partial^2}{\partial \theta^2} + \frac{\epsilon Pr_h \cot\theta}{r_\dagger}\frac{\partial}{\partial \theta} \tag{20}$$

$$\triangle_\psi^* = \frac{1}{H_*^2}\frac{\partial^2}{\partial z_*^2} + \frac{1}{r_\dagger^2}\frac{\partial^2}{\partial \theta^2} - \frac{\cot\theta}{r_\dagger}\frac{\partial}{\partial \theta}. \tag{21}$$

J_* is the nondimensional Jacobian with respect to (z_*, θ), and J_0 is an associated nondimension coefficient dependent on z_* and θ. The domain of computation for all of the results to be reported below is from 80°N to 80°S, and from 0 to 3900m depth (assuming no bottom topography). In terms of the diagnostic fields, stress free conditions for velocity are imposed;$\psi = 0$ is assumed on all boundaries, and $\omega = 0$ is assumed on the north and the south boundaries, where $\omega = u_\theta / r$. As for the prognostic fields, the surface temperature of the ocean strongly influences and is controlled by the atmosphere whereas the surface salinity is influenced by no similar feedback process. Mixed boundary conditions therefore are employed; namely a Dirichlet condition for temperature and a Neumann condition for

the salinity field. A no flux condition on all other boundaries is imposed on both of these fields. In nondimensional form we therefore assume, at $z_* = 1$, that:

$$T_* = Ra_T f_T \tag{22}$$

$$\frac{\partial s_*}{\partial z_*} = Ra_s f_s \tag{23}$$

$$Ra_T = \frac{g\alpha \tilde{T}_c L_z^3 \epsilon_r^2}{\nu K_T} \tag{24}$$

$$Ra_s = \frac{g\beta \tilde{s}_c L_z^3 \epsilon_r^2}{\nu K_T}. \tag{25}$$

f_T and f_s are forcing functions with amplitudes of order 1. $\tilde{T}_c$ and $\tilde{s}_c$ are the actual physical amplitudes of the forcing: $\tilde{T}_c = 14.0[°\mathrm{C}]$, and $\tilde{s}_c = 0.0355$. The nondimensional parameters Ra_T and Ra_s will be recognized as thermal and haline Rayleigh numbers respectively. Figure 1 shows the forcing functions to be employed in the computations when convective adjustment is not utilized.

Because extreme density inversions do develop in the thermohaline flow of interest to us, a convective adjustment scheme may be employed to neutralize each water column in the density field at each time step. At each grid point, the column is scanned from top to bottom, and the layer is mixed where static instability arises. It requires iteration to obtain a fully adjusted column in our scheme, and the number of iterations required was examined by generating randomly distributed columns. The number was found to be dependent on vertical resolution and, for instance, with the 97 vertical grid points employed in most of our calculations the iteration sequence usually converges within 20 iterates but sometimes requires more than 70. We chose the maximum number of iterations to be twice the number of vertical grid points for the calculations in which convective adjustment was employed.

3. NUMERICAL SENSITIVITY

The results from the analyses to be reported here were for the most part obtained on the SGI IRIS 4D/440S computer although one case was integrated on the CRAY Y-MP at the Pittsburgh Supercomputing Center for comparison purposes. The IRIS 4D employs 32bit words, while the Y-MP word is 64bit. Comparison of the results obtained on the two systems revealed that those obtained on the Y-MP were quantitatively similar to those obtained on the IRIS 4D, so that single precision(32bit) arithmetic is clearly adequate. More interesting to us is the fact that the speedup obtained for the code on the Y-MP was only a factor of 9 (single cpu's were employed on each system).

Strong sensitivity to increases of resolution was clearly demonstrated in these preliminary analyses, mainly due to surface boundary layer formation. Figure 3 shows a comparison of cases based upon different vertical resolutions but the same horizontal resolution (all other physical and numerical parameters of the model were held fixed). In these two plates the abscissa is time in kyr, while the ordinate is latitude; contours are of the meridional heat flux.

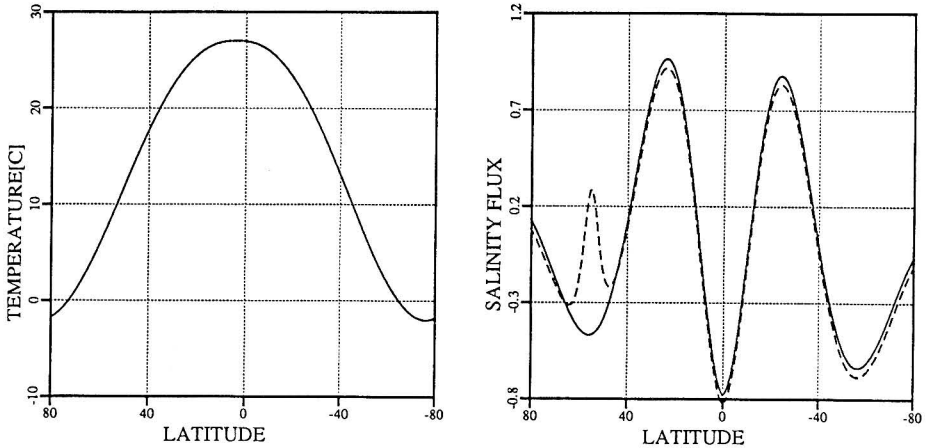

Figure 1: Realistic distributions for temperature(°C , left) and salinity flux (nondimensional, right). The solid line on salinity flux was employed to investigate numerical sensitivity and bifurcation structure, and the dashed line for the investigation of bifurcation structure and for calculations in the realistic regime of parameter space.

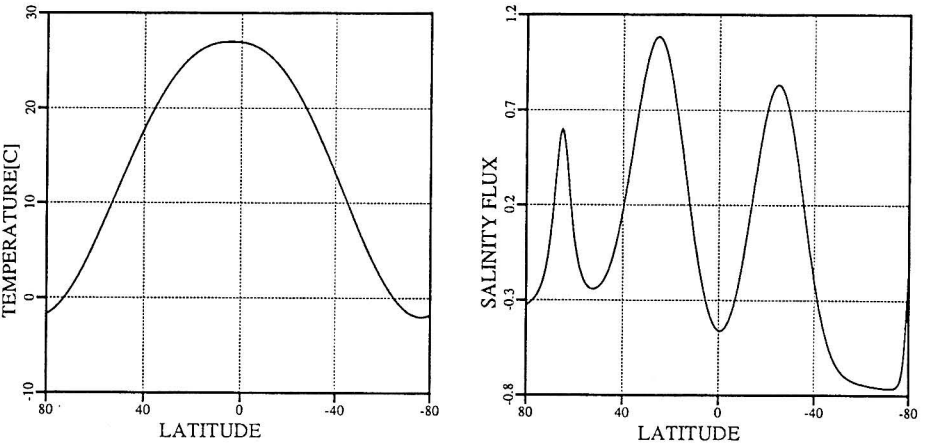

Figure 2: Realistic forcing distributions for temperature(°C, left) and salinity flux (nondimensional, right). This has been employed with a convective adjustment scheme to produce realistic bottom temperature.

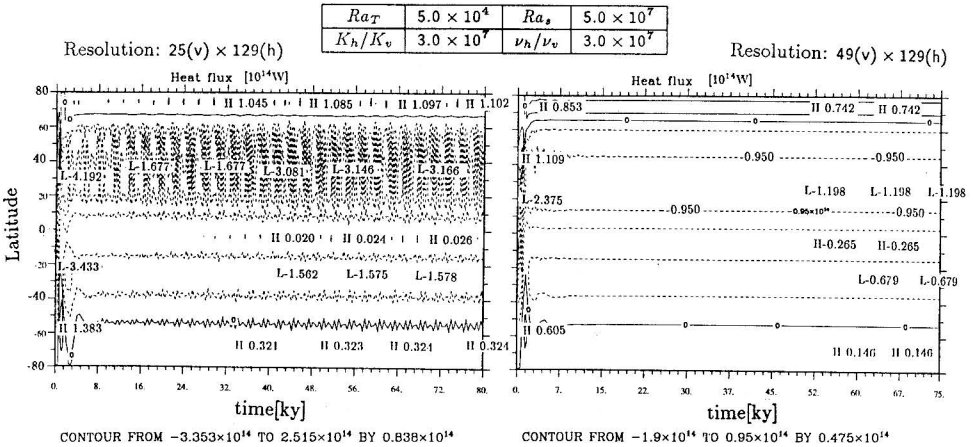

Figure 3: Sensitivity to vertical resolution. The meridional heat flux is contoured in the time(horizontal, in kyr)-latitude(vertical, in degrees) plane, computed with the same control parameters. The coarse resolution model(left) has an oscillatory solution, while the fine resolution model(right) does not.

The coarse resolution result clearly exhibits oscillatory behavior with a period near 2.6 kyr. On the other hand, the fine resolution result exhibits no such oscillation. Even the average strength of the circulation itself is different; that computed with coarse resolution being much stronger than that based upon the fine resolution model. Other numerical sensitivity tests indicate (not shown here) for the case in which a steady state is achieved, that the strength of the circulation is inevitably stronger for the coarse resolution model than for the fine resolution model, although qualitative patterns of flow are similar. Using the uniform grid model, we have found 49 vertical grid points was sufficient to resolve the horizontal thermal and haline boundary layers, these being features that must be adequately resolved if the dynamical behavior is to be realistically described.

Sensitivity to horizontal resolution was also investigated: When the narrow downwelling region of deepwater formation is insufficiently well resolved, numerical instability inevitably arises. This is because the boundary layer structure of the strong downwelling column must also be resolved if an accurate characterization of the mixing process is to be obtained. This sensitivity does not arise in convectively adjusted models, however, since the convective motions are only implicitly represented therein.

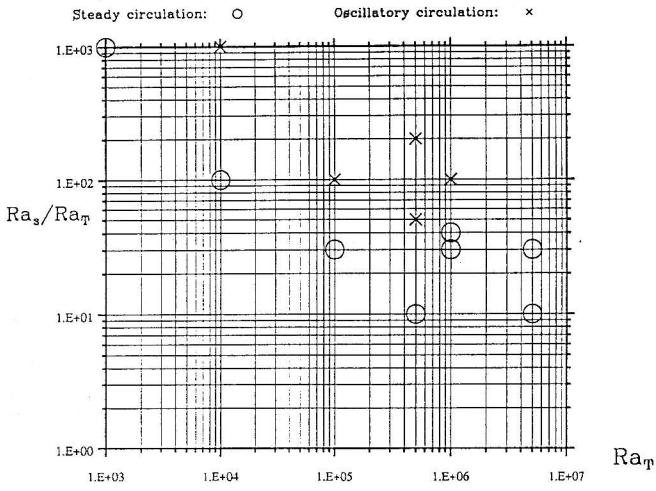

Figure 4: Bifurcation map in the domain of thermal Rayleigh number Ra_T vs the ratio Ra_s/Ra_T, under the salt forcing shown as a solid line in Fig.1. Steady circulations are shown as circles and oscillatory solutions as X. Since the forcing is asymmetric, the steady solution is always of the one-cell type.

4. RESULTS

4.1 Without convective adjustment.

Before performing the main experiments to be described in this paper, we examined the behavior of the model in the regime of relatively small Rayleigh number with symmetric forcing. As shown in Marotzke et al.(1988), and Wright and Stocker(1991), multiple equilibria exist with mixed boundary conditions that consist of unstable two-cell circulations and stable one-cell, pole-to-pole circulations. These stability characteristics appear to disagree with the result of Thual and McWilliams(1992), and the analytical result of Cessi and Young(1992), in which each of the multiple equilibria were shown to correspond to stable states. The latter results were, however, obtained under conditions of very weak forcing, in the thermally dominated regime, whereas our results are for strongly salt-forced flow. Both these previous results are therefore correct in their respective regimes of parameter space.

Our model exhibits a clear transition from time-independent to time-dependent flow as the Rayleigh numbers are increased. Beyond this transition there are no stable equilibria and the model always displays strongly time dependent behavior. This is a consequence of the flux condition on the salinity field at the surface, since no such oscillatory behavior is observed under homogeneous Dirichlet conditions. In general the transition to time-dependent flow is strongly dependent on the haline Rayleigh number, and generally occurs near $Ra_s \sim 10^6$.

Figure 4 presents a regime diagram for flows computed using the surface boundary con-

ditions denoted by the solid lines in figure 1. When the ratio Ra_s/Ra_T is low, it requires high thermal Rayleigh number to achieve oscillatory behavior, while the thermal Rayleigh number may be relatively low in the time-dependent regime when this ratio is high. It is clear from these results that there is a lower limit of the ratio below which no oscillatory mode appears, in which regime the circulation is dominated by the temperature field.

This same transition from steady to oscillatory flow is observed under different forcing conditions (not shown), implying that the bifurcation itself is independent of the detailed properties of the forcing distribution and associated with a local instability. Under asymmetric forcing, a single cell circulation always dominates the oscillation, whereas under symmetric forcing with comparatively low Ra_s/Ra_T (but larger than 10), the oscillation occurs between one-cell type circulations having opposite directions of flow via two cell circulation patterns. Even under symmetric forcing but with larger Ra_s/Ra_T ratio, a single cell circulation always dominates the flow pattern. A typical sequence of events in this mode of oscillatory behavior can been seen in Figure 5: the salinity field indicates that the first oscillatory mode is due to oscillatory downwelling plume formation. A downward plume is being formed at upper mid-latitudes of the northern hemisphere. One residual plume structure will be observed near the ocean floor, while the next episode of plume formation is about to begin at the surface. The label 'H' below the equator denotes a diffusively moderated watermass delivered to depth by the preceding plume found immediately below the surface region of deepwater formation.

The dependence of this bifurcation to oscillatory behavior on the Lewis number has also been examined. A Lewis number larger than unity weakens the circulation when all other parameters are fixed. The larger the number, the weaker the circulation and the weaker the oscillatory mode of behavior. This is a simple consequence of the fact that a lower vertical salt-diffusivity makes the halocline thinner, which eventually causes weaker effective salt forcing even though the forcing at the upper boundary is the same.

Besides this oscillatory mode of behavior associated with episodic plume formation, our analyses have revealed a further oscillatory mode of behavior. Figure 5 in fact exhibits the typical structure that is characteristic of this "dual"-oscillatory mode. The strongest peak in the power spectrum of the meridional heat flux is found to correspond to a period near 400 years with the oscillation localized into the northern hemisphere near the region of deepwater formation corresponding to the primary oscillatory mode. There are also two weaker peaks in the power spectrum at shorter periods, which are considered to be harmonics of the dominant 400 year period, respectively at 200 and 100 year periods. There clearly exist other peaks in the power spectrum and these other peaks are found in the longer period region, near 800 years and 2000 years with much broader power distributions. The peak at 800 years period is possibly associated with period doubling of the dominant mode, but this is not clearly evident in the time series itself that is shown in figure 5. The longer cycle, however, is clearly not the result of period multiplication. In figure 5 we show the time series of the maxima and the minima of the stream function. Other than the dominant variation at 400 years period, there clearly also exist longer timescale and quasiperiodic variations,

which are responsible for the broad peak on the power spectrum in the low frequency regime.

This mode, while the first can always be found under sufficiently high Rayleigh number conditions, has a rather complex relationship to the control parameters. Although we had expected more complex temporal behavior to appear in spectra as the Rayleigh number was increased, this second mode was observed to disappear when the frequency of the first mode was increased sufficiently. Although the spectra of Figure 5 revealed a quite localized second mode, it is often found to cover a much broader band of latitudes.

In Figure 6, for example, we show a result from a calculation in which the horizontal viscosity is 1/100 the magnitude of that employed for the calculation shown in Figure 5. There is false power in the power spectrum from this calculation at high latitudes ranging from 5 kyr to longer period, which is due to the fact that the model time series is still highly non-stationary. The frequency domain appearance of the oscillatory behavior in this example is clearly much more complicated than in the proceeding example. In terms of the first mode, there exist more harmonics as well as the evidence of period doubling. There is irregularity not only in the spectra but also in the heat flux time series and in the maxima and minima of the streamfunction. This suggests that the first mode has began to evolve in a quasi-chaotic manner. The second mode is less sharply defined in the power spectrum than in the case for the example shown in Figure 5, both in period and in latitude. The ratio of peak strengths between the first mode and the second mode was about 6 in Figure 5 while it is near 9 in Figure 6.

It has been found through investigation of the parameter space that the mode on the circulation timescale appears distinct only when the successive episodes of "plume" formation in the downwelling region leave relatively strong density contrast over the basin. Because plume formation is driven by local density gradient and its timescale can be shorter than the horizontal advection timescale when the downwelling region is narrow; the basin scale density contrast acts as another driving force on basin scale flow. If the horizontal density contrast is sufficiently strong, an instability occurs. This instability is analogous to the upper boundary layer instability in the sense that it is caused by imbalance among the supply of heavy water, relaxation due to diffusion, and advection driven by the density forcing. This process appears more clearly in the case with convective adjustment and will be discussed further below.

When we examined the flows characterized by much smaller horizontal viscosity coefficients, we found that the downwelling circulation became narrower and stronger even though the Rayleigh numbers were kept unchanged. This is clearly because the reduced horizontal viscosity makes the watermass in the downwelling region less sluggish and the balance with momentum diffusion is achieved with stronger shear in velocity. Generally speaking, as the horizontal viscosity decreases, this effect weakens the second oscillatory mode, and the first oscillatory mode is found to assume a simpler form (not shown).

In spite of these interesting characteristics, the model without convective adjustment has several unrealistic features. For example, the bottom temperature is too high and it is rather difficult to obtain both realistic circulation strength and a reasonable pattern for

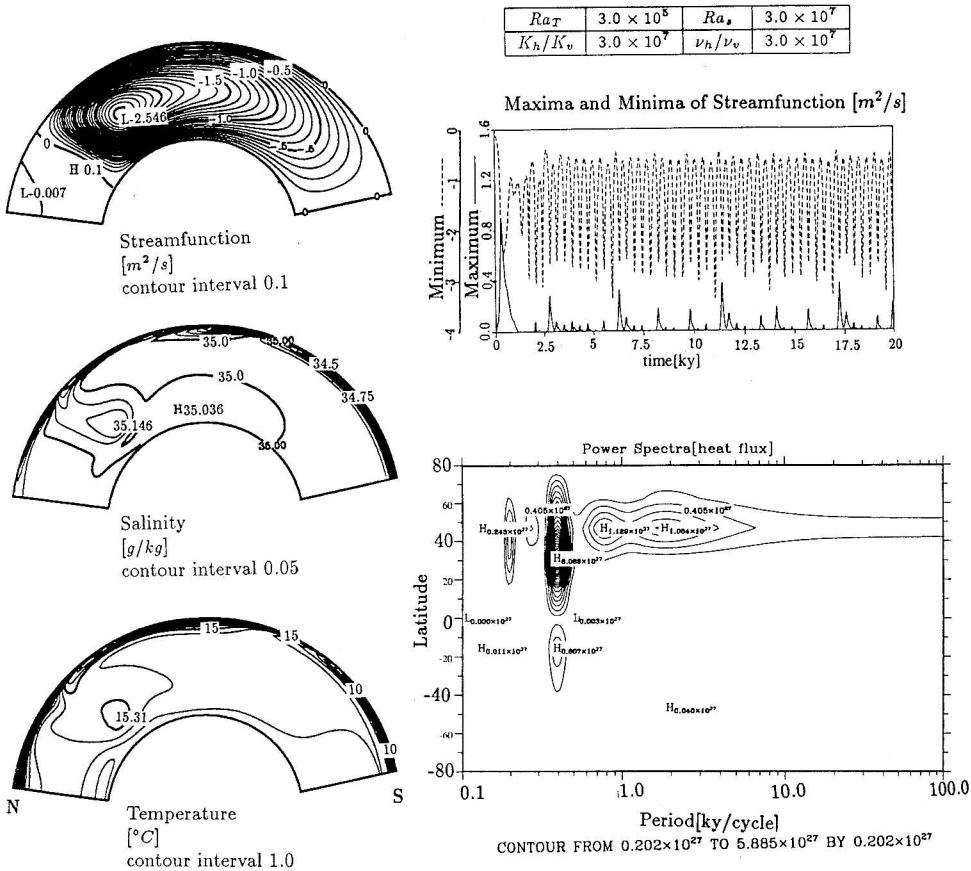

Figure 5: A typical "dual"-mode osillation. The leftmost three figures are streamfunction, salinity and temperature. Also shown is the power spectrum contour map of the time series of meridional heat flux, where the horizontal axis is period (kyr/cycle) and the vertical axis is the latitude in degrees. Also shown is the time series of the maxima (solid line) and the minima (dashed line) of the streamfunction.

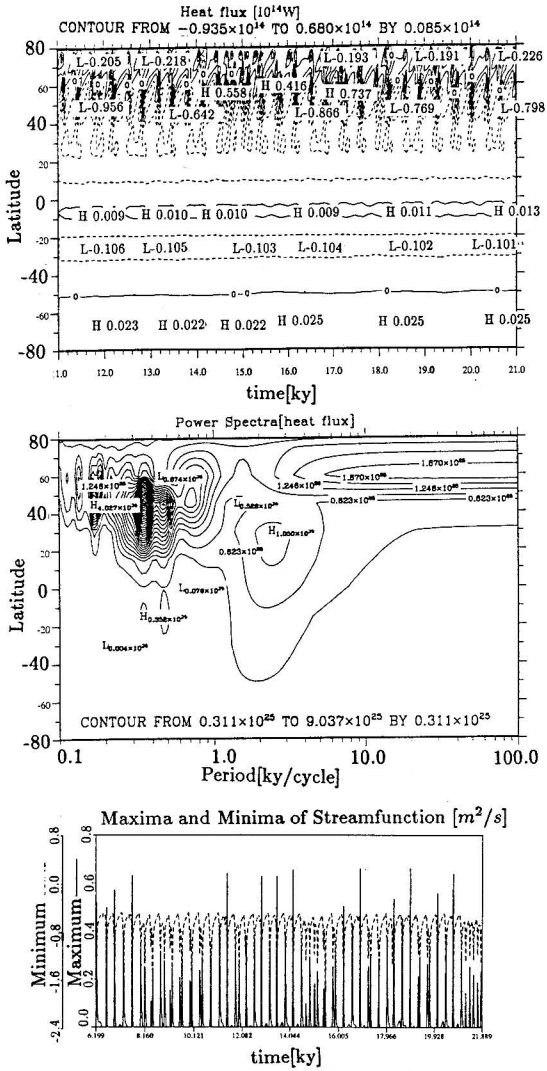

Figure 6: Another "dual"-mode osillation. At the top is shown the time series of meridional heat flux in the time(kyr)-latitude(degree) plane, the middle figure is power spectrum contour map of the time series of meridional heat flux, where the horizontal axis is period (years/cycle) and the vertical axis is latitude distribution. The final plate is the time series of the maxima (solid line) and the minima (dashed line) of the streamfunction.

the distribution of a passive tracer. This is at least partly a consequence of the fact that a linear equation of state for sea water has been employed in these calculations. In the salinity-dominated regime, the heaviest water should be formed at high latitude according to the more accurate nonlinear equation of state when a realistic ratio of thermal and salt forcing are employed. Assuming the horizontal viscosity to be 10^{-4} times that employed in the standard case, and with a high resolution that has 49 grid points in the vertical and 2049 grid points in the horizontal (the grid interval is 11 km), we eventually obtained a vertically uniform field in the downwelling region for a passive tracer, but a circulation that is still weaker than observational constraints demand. A model with such high resolution costs as much as a three-dimensional model to run, and is clearly impractical for the long integrations required to address problems in paleoclimatology.

It is of course possible to increase the strength of the circulation by simply modifying the redimensionalization; chosing $K_{Tv} = 10^{-4}[\mathrm{m}^2/\mathrm{s}]$ will raise the circulation strength from 1.5 Sv to 15 Sv. At the same time the period of the first oscillatory mode will become 10 times shorter, because the redimensionalization is determined by the characteristic time scale of K_{Tv}: a period of 2 kyr therefore become 200 years.

4.2 With convective adjustment.

By employing a convective adjustment scheme, the performance of our non-hydrostatic model was considerably improved. The implicit convective motion that controls the deepwater formation process then becomes disconnected from basin scale flow, and it is horizontal advection that produces vertical motion in order to ensure continuity. In order to achieve a realistic circulation strength, we fixed both the vertical and horizontal resolution at 97 grid points. The nonlinear equation of state described by Fofonoff(1985) that is based upon experimental data was also employed for the purpose of these analyses. The forcing employed for these simulations (Fig.2) is slightly different from that employed for the analyses discussed in the preceding section, but the basic shape of the functions is similar. With these modifications the bottom water temperature decreases to a value near that of the surface in the region where deep water is formed and we obtain a much better fit to observational data.

A series of investigations in the parameter space of this more refined model made it clear that there again exists at least two characteristic modes of oscillatory behavior. One of them was found to be explained by an identical process to that found in the model without convective adjustment, but the other appears to be an artifact of the convective adjustment procedure.

Firstly, the slow oscillation on the time scale of the circulation itself is again observed when the Rayleigh numbers are sufficiently high. This is directly driven by the process whereby the dense mass of deepwater extending through a vertically uniform column is formed. This downwelling "plume" can be seen clearly on Fig.7. On both the temperature and the salinity fields of this figure we observe the signature of the pulsation: the next bubble of deepwater is being formed at the base of the downwelling region at high northern latitudes, and the previous pulse is observed to have moving southwards along the sea floor.

Ra_T	4.0×10^5	Ra_s	3.2×10^6
K_h/K_v	3.0×10^7	ν_h/ν_v	3.0×10^5

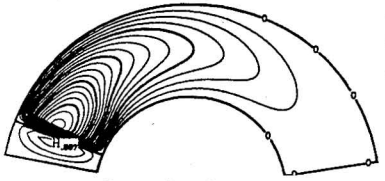

Streamfunction
$[m^2/s]$
contour interval 0.04

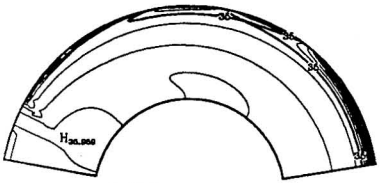

Salinity
$[g/kg]$
contour interval 0.25

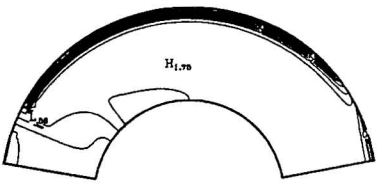

Temperature
$[°C]$
contour interval 1.0

N S

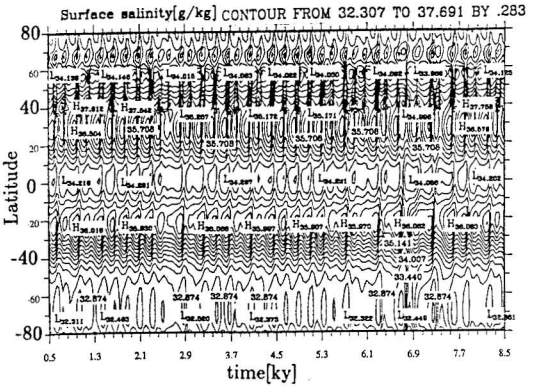

Bottom-Average Salinity

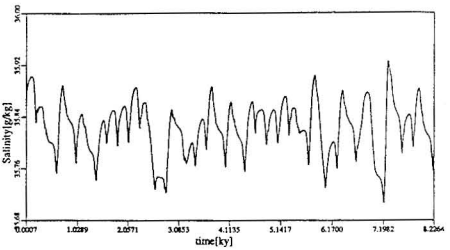

Bottom-Average Temperature

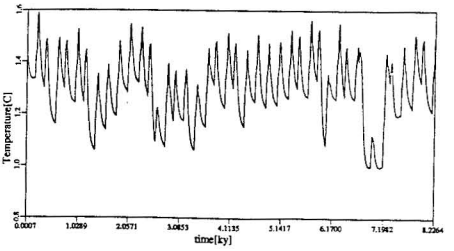

Figure 7: The themohaline circulation in the realistic regime with a convective adjustment scheme.

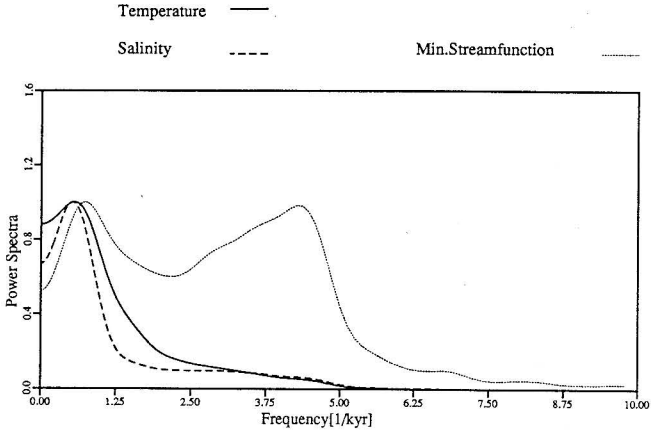

Figure 8: The power spectrum of bottom average temperature, salinity, and maxima and minima of the streamfunction. This calculation was carried out using the Rayleigh numbers; $Ra_T = 1.0 \times 10^4$, $Ra_s = 1.0 \times 10^5$, which are about 1/30 as small as that of shown as the example in the realistic regime.

The fundamental mechanism underlying this process is exactly the same mechanism as that discussed in the preceding section concerning the oscillation on the circulation timescale, but here it is observed more clearly. At steady state, a relatively heavy watermass remains below the downwelling region and extending equatorwards, with the location of individual isopleths determined by the balance between advection and diffusion. Additional salty and cold water at the latitude of the downwelling region strengthens the density gradient which drives the horizontal circulation. The locally enhanced flow then "stretches" the plume southwards. As the plume moves horizontally, the horizontal density gradient relaxes and the flow weakens. After a plume is sufficiently "stretched" that the circulation is not strong enough to support it, diffusion rapidly erodes the thin stem of the southward moving plume until the next accumulation of heavy water at the downwelling region starts.

The second oscillatory mode of behavior in the model with convective adjustment is characterized by chaotic but relatively weak variability which contains very high frequency components. Fig.8 shows the power spectrum of bottom average temperature and salinity and maxima and minima of the streamfunction from the result computed with smaller values of the Rayleigh numbers such that the oscillation on the timescale of the circulation is no longer prominent and this chaotic noise is shown more clearly than in the example from the realistic regime. These features can easily be found in the bottom average temperature and salinity, and maxima and minima of streamfunction. The power spectra of these time series display red-noise like in the decade to millennium structure band. The circulation timescale mode is affected by this high frequency noise, especially the bottom average temperature

and salinity which now oscillate irregularly.

An *a posteriori* estimation of the Taylor number for these flows has also been performed. The Taylor number is of course defined as the ratio of the Coriolis force to the horizontal viscous force. In order to obtain this estimate, the Prandtl number is set such that the ratio of the inertial force to the buoyancy force is at most 10^{-2} so as to satisfy Hasselmann's(1982) argument for the neglect of the inertial force. The Taylor numbers thereby found to be characteristic of our thermohaline flows range from 10^{-2} to 10^{2} when the strength of the thermohaline circulation is in the realistic regime. In general, the weaker the circulation, the lower the Taylor number. It is quite clear on the basis of these *a posteriori* analyses that the neglect of the Coriolis force on the overturning circulation may well be justified, although there still remains uncertainty in this regard.

5. DISCUSSION

Three distinct Oscillatory modes of behavior have been observed in the numerical integrations of the thermohaline circulation system reported here. The first is observed only in the case without convective adjustment, the second is found in cases both with and without convective adjustment, and the third mode appears to be entirely due to the convective adjustment scheme.

Firstly, the oscillatory mode driven by explicitly resolved convection will quite likely occur in the real ocean given its characteristic vertical diffusivity. This mode is driven by boundary layer instability which must occur several times per year, each event lasting of order of a week, and being confined to a very localized region (e.g. Hakkinen et al.,1992). The frequency, however, would not relate to that of our model: The fixed boundary value/flux condition at the surface on temperature/salinity is apparently inadequate to correctly describe such a short timescale phenomenon. Supposing that each such convective event is so rapid and spatially localized that the physical properties in that scale may be rendered uniform, such convective downwelling events are clearly quite distinct from basin scale activity. In this limit, the process of convective downwelling may clearly be replaced by convective adjustment.

Secondly, the century scale oscillation driven by the horizontal density gradients could well be the origin of the climatic oscillation reported by Stuiver(1980). This process is generated not only by our model but also by the OGCM of Mikolajewicz and Meier-Reimer(1990) although these authors found the century scale oscillation to be revealed as a response to externally applied stochastic forcing. If this process actually occurs in the Atlantic Ocean, there must be some signature in the salinity and temperature fields. It is not clear, from the existing observational data of Levitus(1982) whether or not the Atlantic Ocean basin contains any signature of watermass pulsations or not at present, although the data is based upon observations spanning only decade. Further modern observational data or more dense coverage by paleoclimatic data would be necessary for validation of this mode of oscillatory behavior.

Thirdly, the red-noise like fluctuations are probably driven by the interaction between

convective adjustment and the basin scale flow. Although similar interaction between basin scale flow and the region where deep convection occurs may exist in reality, a convective adjustment scheme essentially represents an *ad hoc* treatment of a subgrid scale process and thus the details of the behavior produced by including the scheme may be spurious. Validation through the use of a fully resolved deep convection model would therefore be required. Assuming that this noisy behavior is physically significant, it would, however, be difficult to distinguish any signature of the chaotic behavior of the long timescale oscillation within existing climatic records, for it is clearly the case that the ocean is not the only source of stochastic variability in the climate system.

The mode of oscillatory behavior produced by the model of Winton and Sarachik(1993) is not found in our model. Their model oscillates under certain conditions with century timescale and, of special interest from the perspective of the Dansgaard-Oeschger oscillations, with millennium timescale, which they explain to be due to different mechanisms. The shorter periodicity appearing in their model may be identical with our oscillatory mode on the characteristic time scale of the circulation. The timescale of their second mode is very close to the characteristic time of vertical diffusion.

The millennium timescale oscillation might be implicated in the Younger-Dryas interruption of the last deglaciation, but is less possible as an explanation of the Dansgaard-Oeschger oscillations which persist in the modern record. This is because their sequence of oscillatory modes is characterized by two drastically different stages of flow patterns, which is not reported in observational data: in the longer part of the cycle the flow is weak with very shallow surface circulation and the deep layer remains essentially stagnant. This flow is replaced periodically by very short, violent and deep overturning events. On the basis of these results, the net surface freshwater input is positive, but localized negative input exists to cause strong downwelling.

Our model has not yet provided any clear explanation for this millennium scale climatic oscillation. The chaotic variability may temporarily produce patterns which look oscillatory on the millennium scale, but this is not a particularly convincing suggestion. One possible explanation that could be developed from our model is one that involves multibasin effects. It is quite clear on the basis of OGCM simulations (e.g. Semtner and Chervin,1992) that the thermohaline circulation interconnects the major ocean basins with deep water forming in the North Atlantic and flow through the Southern Ocean into the Pacific ocean. Combining these basins clearly increases the total volume of interacting water and this lengthens the characteristic timescale of the thermohaline circulation. Might such interconnectivity provide an explanation of the Dansgaard-Oeschger oscillations? This is an issue we are currently attempting to address.

6. CONCLUDING REMARKS

A two dimensional spherical thermohaline circulation model has been developed to investigate the physics of this process. In this model the behavior of the circulation is controlled by

several nondimensional numbers, the most important of which are the thermal and haline Rayleigh numbers. The model ignores the influence of rotation, the relevance of which to the thermohaline overturning circulation remains unclear.

Several important dependences were revealed by our sensitivity analyses; the resolution of the model must be fine enough to resolve the boundary layers formed at the ocean surface whose instability is responsible for the formation of vertical downwelling plumes. For example, insufficient vertical resolution was shown to lead to the appearance of unphysical oscillatory modes of behavior.

There exist three oscillatory modes of dynamical evolution that have been revealed by the preliminary analyses that we have performed. One, that appears in the model without convective adjustment, is related to the plume formation process caused by boundary layer instability. The second mode is driven by horizontal density contrast. Horizontally moving watermass pulses are formed at the base of the column where deep water is formed, and these are transferred advectively to the south. This process is rather similar to the first mode, and the vertically uniform column plays a similar role to that played by the top boundary layer. This mode has been observed both with and without convective adjustment. The third mode appears to consist of red-noise type like variability, and is clearly related to the convective adjustment. This also affects the second mode in the model with convective adjustment and it modifies its period.

To produce realistic distributions of salinity and temperature we have found that the nonlinear equation of state for sea water is necessary and convective adjustment is required for practical reasons. Adding the convective adjustment scheme allows us to obtain a realistic strength for the themohaline circulation with reasonably low resolution. The model then delivers century scale oscillations and some high frequency chaotic behavior. It is suggested that climate variability on shorter than a millennium timescale can be connected to this internal oscillatory mode of behavior.

The mechanism underlying the so-called Dansgaard-Oeschger oscillations is still obscure. Since the characteristic time scale of the thermohaline circulation of the Atlantic basin estimated from both models and observations is less than a millennium, it is difficult to attribute the cause of the Dansgaard-Oeschger variability to this mechanism within the basin although the convection related red noise may provide occasional quasi-millennium scale activity. The operation of the full inter-basin conveyer belt is a possible candidate because the increase in length scale increases the characteristic timescale of the deep circulation.

Our model has succeeded in producing reasonably realistic deep circulation and tracer field patterns despite the complete neglect of the wind driven gyre circulation. The model will be further developed for use in the simulation of ice age climatic change, specifically for incorporation into the model of the ice age cycle of Deblonde and Peltier(1991).

7. REFERENCES

Boyle,E.A. and L.Keigwin(1987) : North Atlantic thermohaline circulation during the past 20,000 years linked to high-latitude surface temperature. *Nature,* **330**:35-40.

Broecker,W.S. and J.Van Donk(1970) : Insolation changes, ice volumes, and ^{18}O record in deep sea cores. *Rev.Geophys.,* **8**:169-198.

Bryan,F.(1986) : High-latitude salinity effects and interhemispheric thermohaline circulations. *Nature,***323**:301-304.

Cessi,P. and W.R.Young(1992) : Multiple equilibria in two dimensional thermohaline circulation. *J.Fluid Mech.,*in press.

Charles,D.C. and R.G.Fairbanks(1992) : Evidence from Southern Ocean sediments for the effect of North Atlantic deep-water flux on climate. *Nature,***355**:416-419.

Dansgaard,W., S.J.Johnson, H.B.Clausen, D.Dahl-Jensen, N.Gundestrup, C.U.Hammer, H.Oeschger(1984) : North Atlantic climatic oscillations revealed by deep Greenland ice cores, in *Climate Processes and Climate Sensitivity,* J.E.Hansen and T.Takahashi(eds.), Geophysical Monograph 29, A.G.U.Press, Washington, D.C.,pp.288-298.

Deblonde,G and W.R.Peltier(1991) : Simulations of continental ice sheet growth over the last glacial-interglacial cycle: Experiments with a one-level seasonal energy balance model including realistic geography. *J.Geophys.Res.,***98**:9189-9215.

Duplessy,J.-C., L.Labeyrie, A.Juillet-Leclerc, F.Maitre, J.Dupart, M.Sarnthein(1991) : Surface salinity reconstruction of the North Atlantic Ocean during the last glacial maximum. *Oceanologica acta,* **14**:311-323.

Fofonoff,N.P.(1985) : Physical property of seawater: A new salinity scale and equation of state for seawater. *J.Geophys.Res.,***90**:3332-3343.

Ghil,M., and H.Le Treut(1981) : A climate model with cryodynamics and geodynamics. *J.Geophys.Res.,* **86**:5262-5270.

Häkkinen,S., G.L.Mellor, and L.H.Kantha(1992) : Modeling deep convection in the Greenland Sea. *J.Geophys.Res.,* **97C**:53895408.

Hasselmann, H(1982) : An ocean model for climate variability studies. *Prog. Oceanog.,* **11**:69-92.

Hays,J.D., J.Imbrie and N.J.Shackleton(1976) : Variations in the Earth's orbit: Pacemaker of the ice ages. *Science,***194**:1121-1132.

Imbrie,J.,E.A.Boyle,S.C.Clemens,A.Duffy,W.R.Howard,G.Kukla,J.Kutzbach, D.G.Martinson, A.McIntyre, A.C.Mix, B.Molfino, J.J.Morley, L.C.Peterson, N.G.Pisias, W.L.Prell, M.E.Raymo, N.J.Shackleton, and J.R.Togweiler(1991) : *The structure of major glacial cycles* and *Conceptual model of major Pleistocene glaciation cycles.* by personal communication from Prof. John Imbrie to Prof.W.R.Peltier.

Kutzbach,J., and P.J.Guetter(1986) : The influence of changing orbital parameters and surface boundary conditions on climatic simulations for the past 18,000 years. *J.Atmos.Sci.,* **43**:1726-1759.

Hyde,W.T., and W.R.Peltier(1987) : Sensitivity experiments with a model of the Ice Age cycle: the response to Milankovitch forcing. *J.Atmos.Sci.* **44**:1351-1374.

Lorius,C., J.Jouzel, C.Ritz, L.Merlivat, N.I.Barkov, Y.S.Korotkevich, and V.M.Kotlyakov(1985) : A 150,000 year climatic record from Antarctica. *Nature***316**:591-596.

Manabe,S., and A.J.Broccoli(1985) : The influence of continental ice sheets on the climate of an ice age. *J.Geophys.Res.,* **90**:2167-2190.

Marotzke,J., P.Welander and J.Willebrand(1988) : Instability and multiple equilibria in a meridional-plane model of the thermohaline circulation. *Tellus,***40A**:162-172.

Mikolajewicz,U. and E.Meier-Reimer(1990) :Internal secular variability in an ocean general circulation model. *Clim. Dynam.,* **4**:145-156.

Olbers,D.J., M.Wenzel, and J.Willebrand(1985) : The influence of North Atlantic circulation patterns from climatological hydrographic data, *Rev. Geophys.,* **23**:313-356.

Oeschger,H., J.Beer, U.Seigenthaler, B.Stauffer, W.Dansgaard, and C.C.Langway(1984) : Late glacial climate history from ice cores, in *Climate Processes and Climate Sensitivity,* op.cit., pp.299-306.

Saltzman,B.(1987) : Carbon dioxide and the $\delta^{18}O$ record of late-Quarternary climatic change: a global model. *Clim.Dyn.,* **1**:77-85.

Semtner,Jr.A.J. and R.M.Chervin(1992) : Ocean general circulation from a global eddy-resolving model. *J.Geophys.Res.,* **97C**:5493-5550.

Stocker,T.F. and D.G.Wright(1991) : Rapid transition of the ocean's deep circulation induced by changes in surface water fluxes. *Nature,***351**:729-732.

Stommel,H.M.(1961) : Thermohaline convection with two stable regimes of flow. *Tellus,***XIII(2)**: 224-230.

Stuiver,M.(1980) : Solar variability and climatic change during the current millennium. *Nature,* **286**:868-871.

Thual,O and J.C.McWilliams(1991) : The catastrophe structure of thermohaline convection in a two dimensional fluid model and a comparison with low order box model. *Geophys.Astrophys.Fluid Dyn.,***64**:67-96.

Winton,M. and E.S.Sarachik(1993) : Thermohaline oscillations induced by strong steady salinity forcing of ocean general circulation model. *J.Phys.Oceanogr.,* in press.

Wright,D.G. and T.F.Stocker(1991) : A zonally averaged ocean model for the thermohaline circulation. Part I: Model development and flow dynamics. *J.Phys.Oceanogr.,* **21**:1713-1724.